

## Electronic Supplementary Information

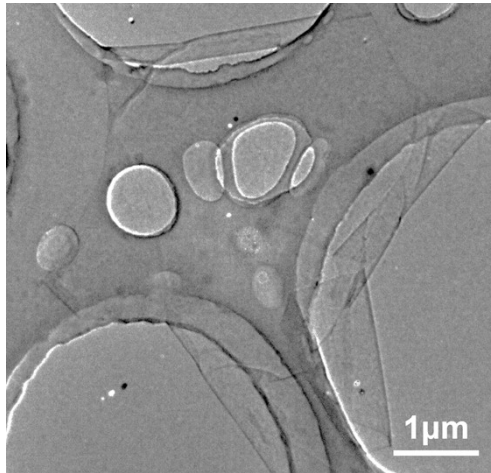
### **Highly Salt-Resistant and Efficient Dynamic Janus Absorber Based on Thermo-Responsive Hydroxypropyl Cellulose**

Jianfeng Gu, ‡<sup>a</sup> Zhaohui Luan, ‡<sup>a</sup> Xinmin Zhang, <sup>a</sup> Huihui Wang, <sup>a</sup> Xu Cai, <sup>a</sup> Weiqing Zhan, <sup>a</sup> Xinyi Ji, \*<sup>a</sup> Jiajie Liang \*<sup>a,b</sup>

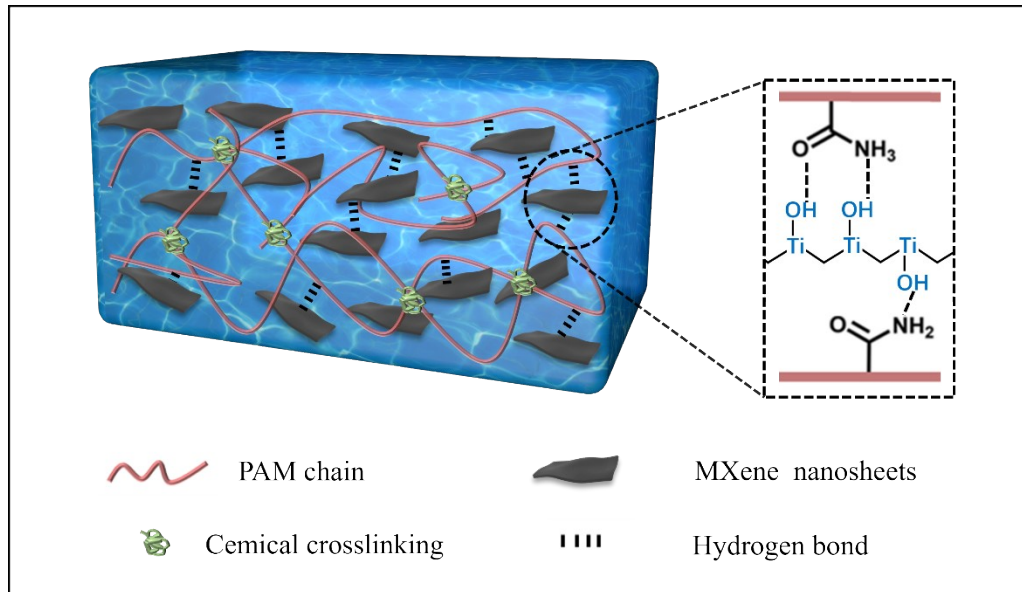
<sup>a</sup> School of Materials Science and Engineering, National Institute for Advanced Materials, Nankai University, Tianjin 300350, China.

<sup>b</sup> Key Laboratory of Functional Polymer Materials of Ministry of Education, College of Chemistry, Nankai University, Tianjin 300350, China.

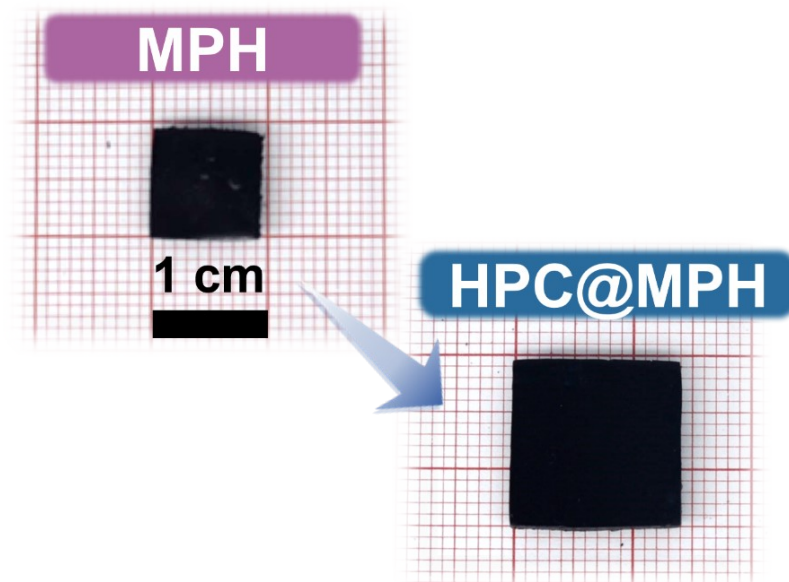
\*E-mail: liang0909@nankai.edu.cn (J. Liang); xyji06@nankai.edu.cn (X. Ji);



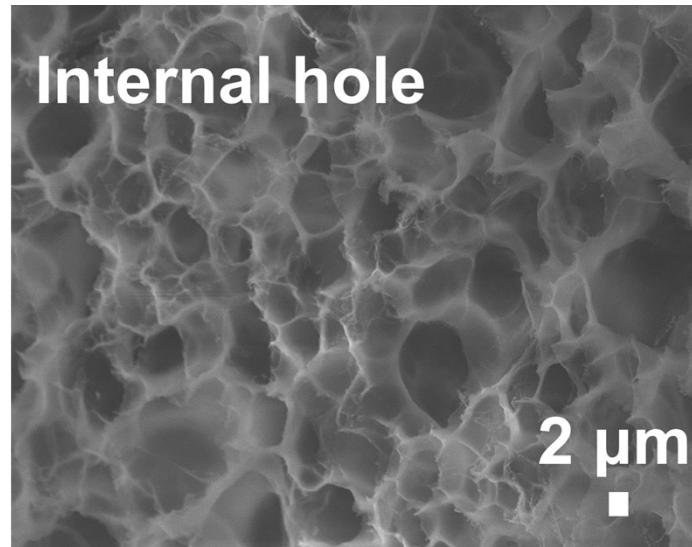
**Figure S1.** TEM images of MXene nanosheets.  $\text{Ti}_3\text{C}_2\text{T}_x$  MXene nanosheets with a lateral size of about  $3.5 \mu\text{m}$  were obtained by selectively etching the Al layer from bulk  $\text{Ti}_3\text{AlC}_2$  MAX, followed by subsequent exfoliation.



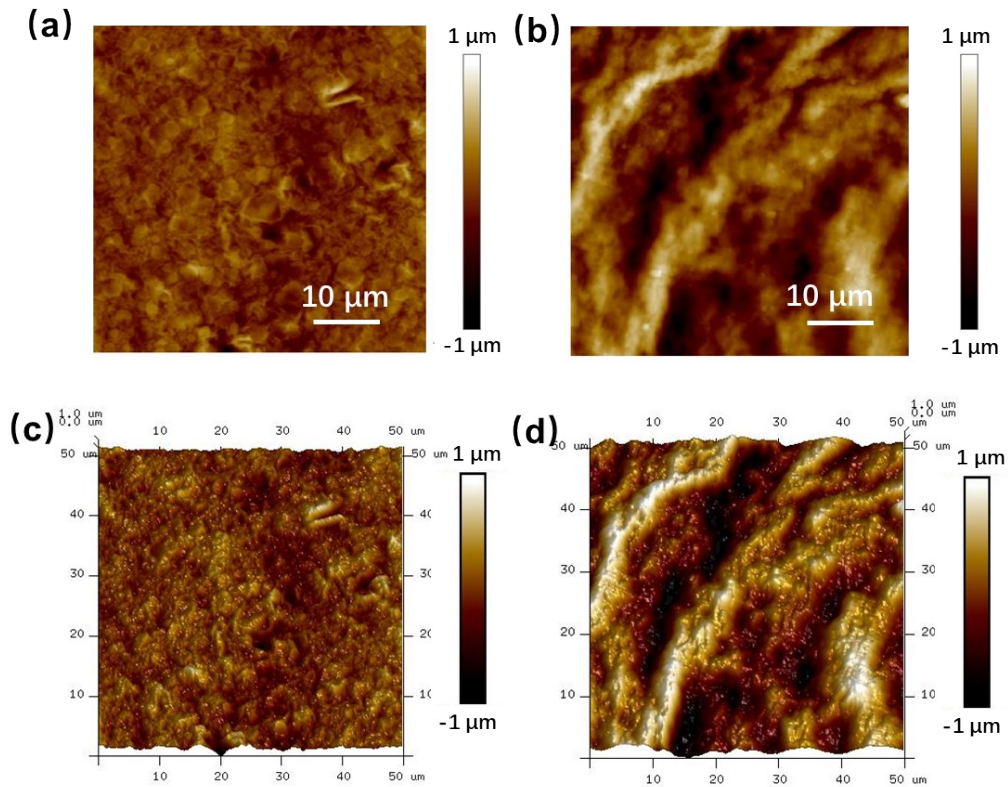
**Figure S2.** Schematic illustration of the structure of the MPH hydrogel.



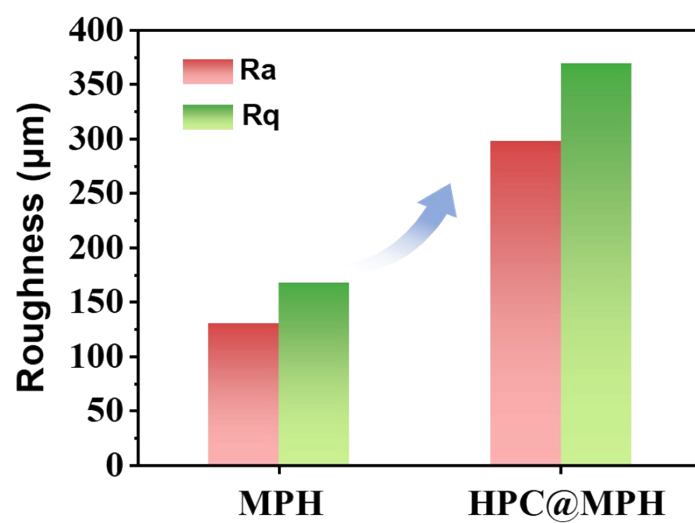
**Figure S3.** The photographs of the MPH and HPC@MPH, respectively.



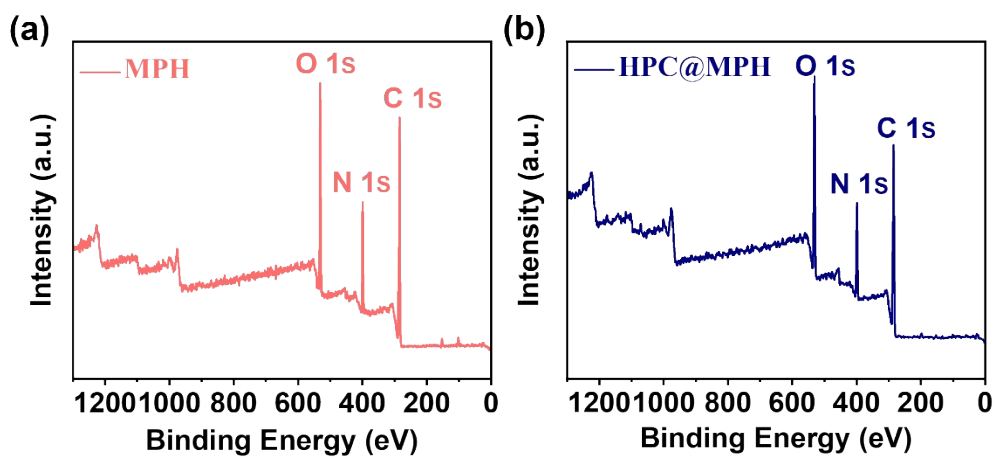
**Figure S4.** Cross-sectional SEM images of the MPH.



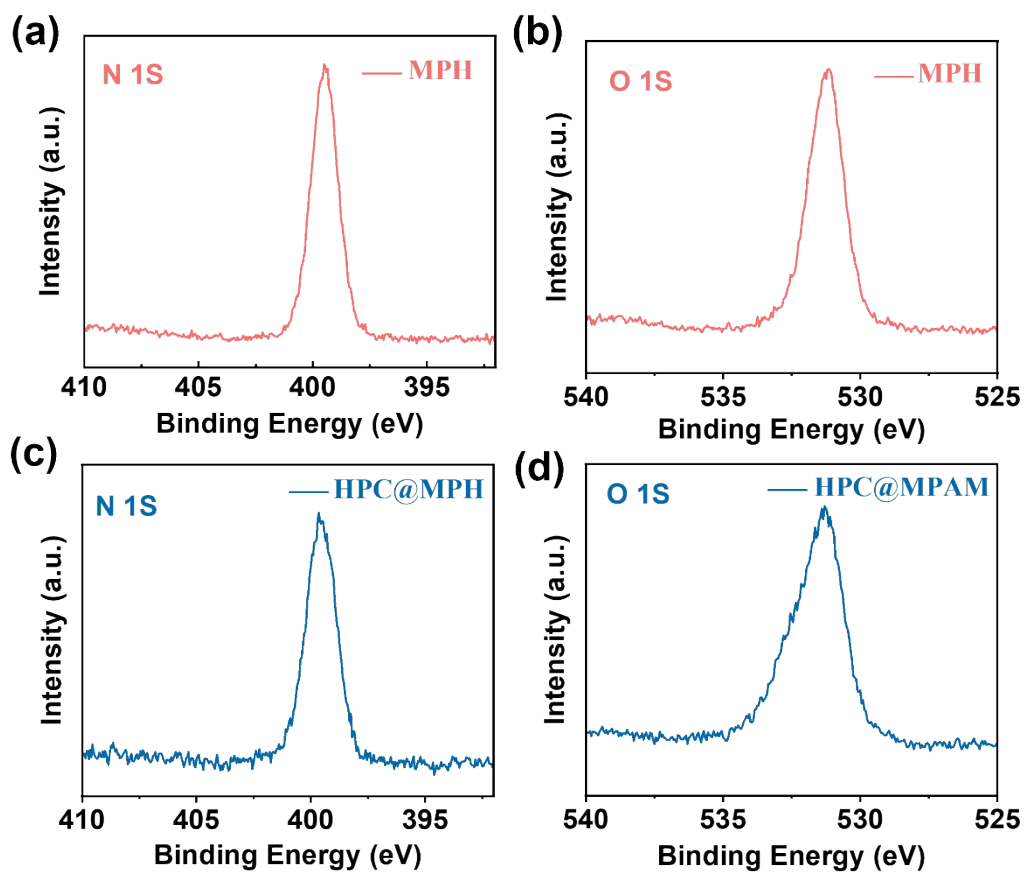
**Figure S5.** a) and b) AFM images of MPH hydrogel and HPC@MPH hydrogel, respectively. c) and d) Visualization of 3D AFM topographic images of the MPH hydrogel and HPC@MPH hydrogel, respectively.



**Figure S6.** The roughness of the hydrogel and HPC@MPH hydrogel, respectively.

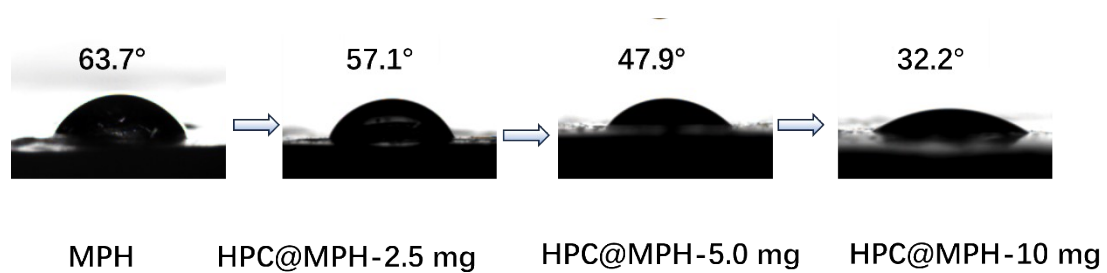


**Figure S7.** The XPS survey spectrum of (a) MPH and (b) HPC@MPH.




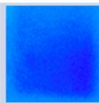
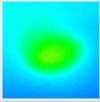
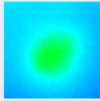


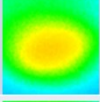
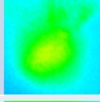
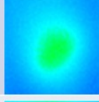

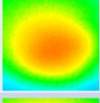
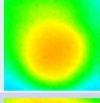
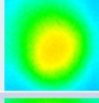

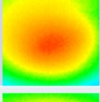
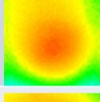
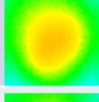

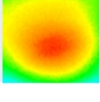
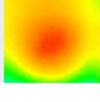
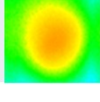
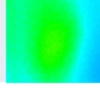


**Figure S8.** The N 1s and O 1s spectrums of the MPH and HPC@MPH, respectively.

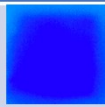

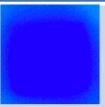
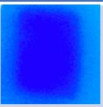
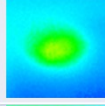
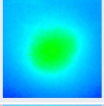


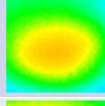
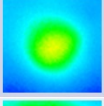
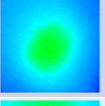
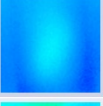
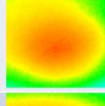
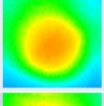
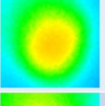
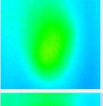
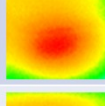
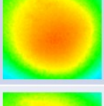
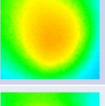
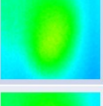
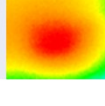
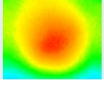
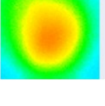
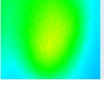




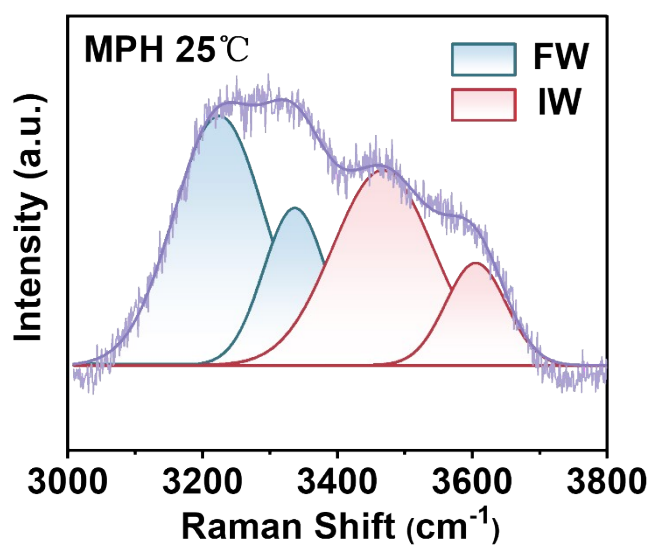
**Figure S9.** The contact angle changes of MPH surface modified by different HPC contents (2.5 mg, 5.0mg and 10 mg).

	0°	30°	45°	60°
0 min	 19.6°C	 19.4°C	 19.6°C	 20.5°C
0.5 min	 31.8°C	 30.3°C	 27.0°C	 25.8°C
1 min	 35.1°C	 32.6°C	 30.0°C	 27.0°C
3 min	 38.3°C	 36.5°C	 34.5°C	 29.7°C
5 min	 39.5°C	 39.0°C	 35.7°C	 31.1°C
7 min	 40.0°C	 39.7°C	 37.2°C	 31.3°C

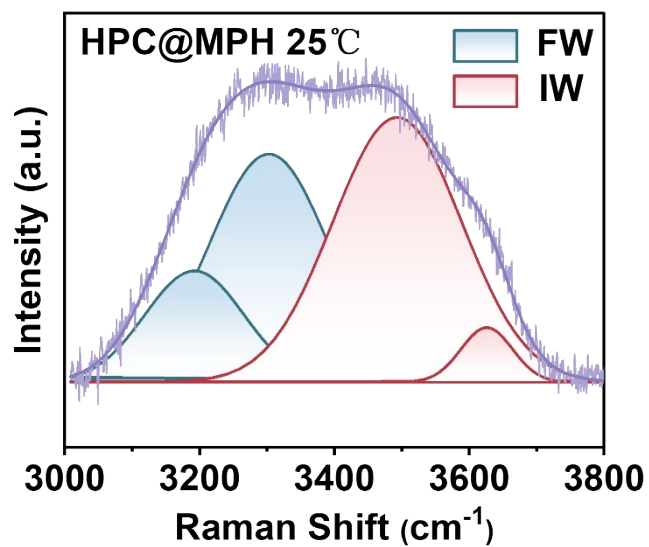
**Figure S10.** Infrared thermal images and temperatures of the MPH at incident angles of 0°, 30°, 45°, and 60° under one sun solar irradiation.

	0°	30°	45°	60°
0 min	 19.6°C	 19.2°C	 19.1°C	 19.5°C
0.5 min	 32.2°C	 30.8°C	 27.6°C	 26.6°C
1 min	 35.8°C	 32.9°C	 30.5°C	 27.5°C
3 min	 39.0°C	 37.2°C	 35.3°C	 31.7°C
5 min	 40.7°C	 38.7°C	 36.4°C	 32.2°C
7 min	 41.4°C	 40.2°C	 38.0°C	 32.8°C

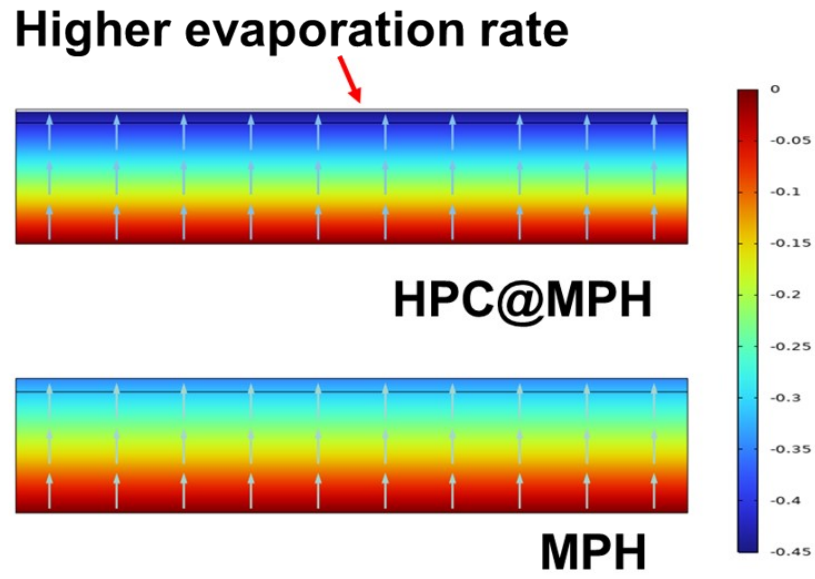
**Figure S11.** Infrared thermal images and temperatures of the HPC@MPH at incident angles of 0°, 30°, 45°, and 60° under one sun solar irradiation.



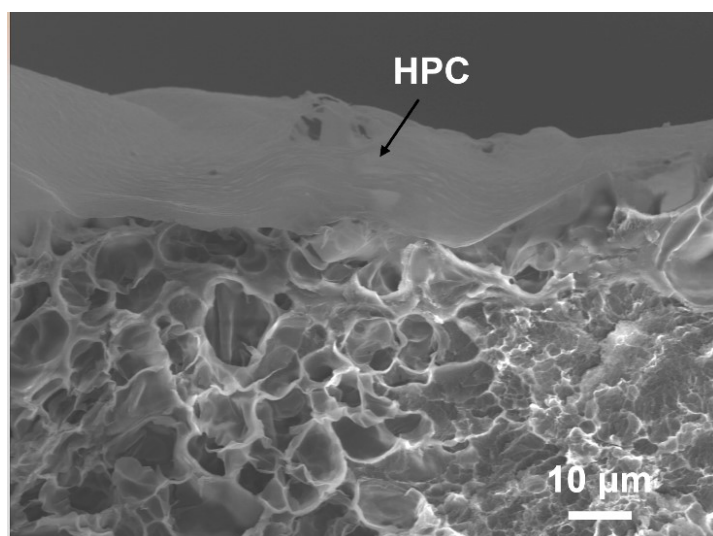
**Figure S12.** Raman spectra showing the fitting peaks representing IW and FW in the MPH at 25 °C.



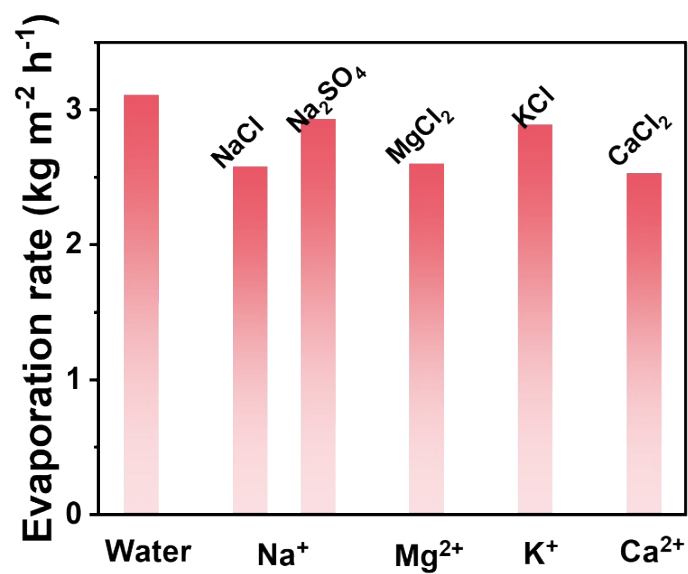
**Figure S13.** Raman spectra showing the fitting peaks representing IW and FW in the HPC@MPH at 25 °C.



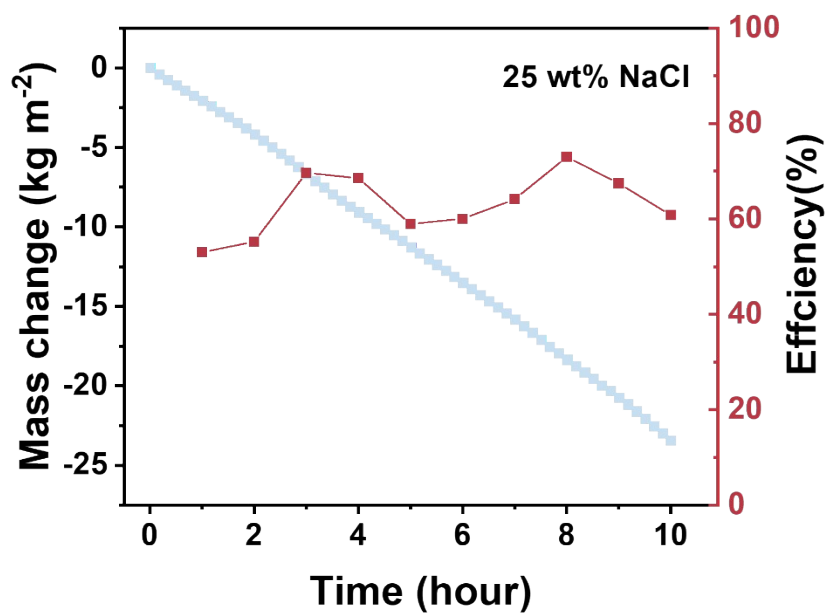
**Figure S14.** The water evaporation rate of MPH and HPC@MPH obtained by COMSOL simulation under one solar irradiation.



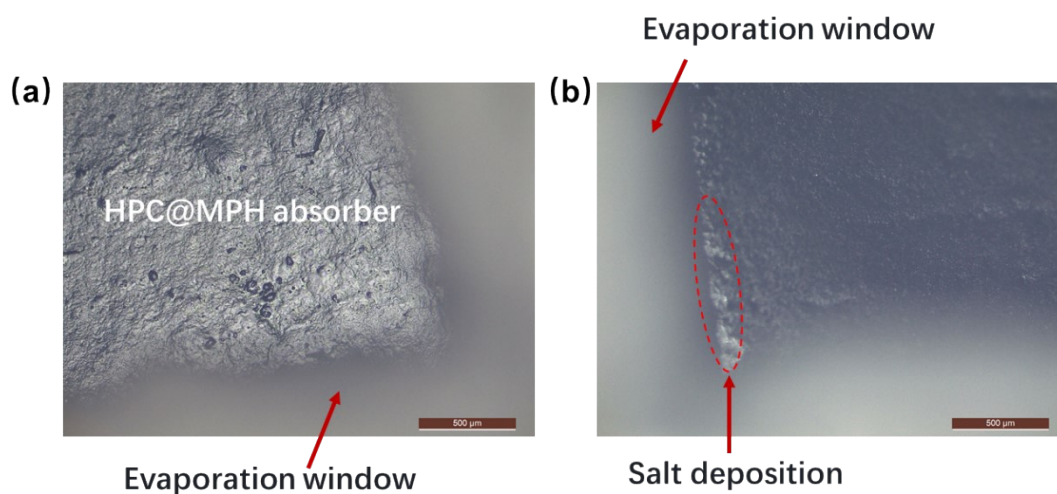
**Figure S15.** Cross-sectional SEM images of the HPC@MPH-10 mg absorbers.



**Figure S16.** Evaporation rates of HPC@MPH absorber in different salt solutions (3.5 wt% NaCl, KCl, MgCl<sub>2</sub>, CaCl<sub>2</sub> and Na<sub>2</sub>SO<sub>4</sub>).

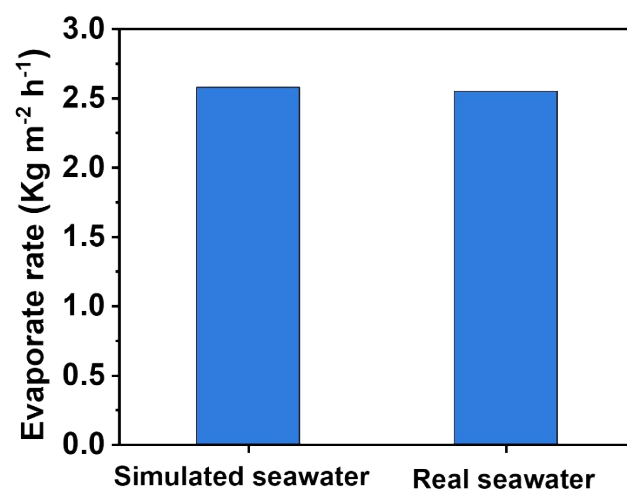


**Figure S17.** Changes in mass and evaporation efficiency of the HPC@MPH evaporator tested in 25 wt% NaCl simulated seawater.

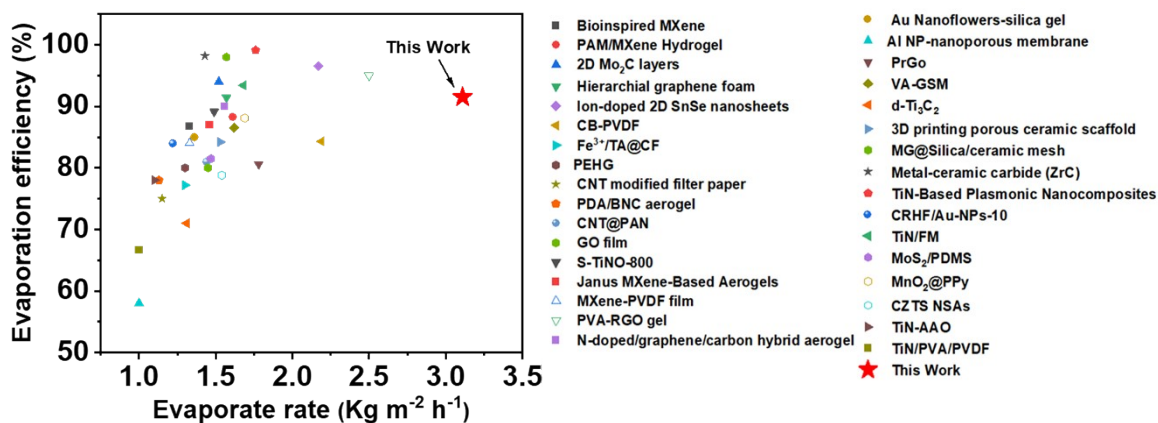


**Figure S18** a and b) The salt deposition images of the HPC@MPH evaporator after 1 - hour and 10 - hour water evaporation tests in a 25 wt% NaCl solution.





**Figure S19.** The performance comparison of the average evaporation rate of the HPC@MPH absorber in simulated seawater and real seawater.



**Figure S20.** The comparison of the evaporation efficiency and evaporation rate of the previous materials.

**Table S1** The comparison of the evaporation efficiency and evaporation rate of the previous advanced materials under  $1 \text{ kW m}^{-2}$ .

Materials	Evaporate rate ( $\text{Kg m}^{-2} \text{h}^{-1}$ )	Evaporation efficiency (%)	Ref.
Bioinspired MXene	1.33	86.7	1
PAM/MXene Hydrogel	2.61	88.3	2
2D $\text{Mo}_2\text{C}$ layers	1.52	94.0	3
Hierarchical graphene foam	1.57	91.4	4
Ion-doped 2D SnSe nanosheets	2.17	96.5	5
CB-PVDF	2.19	84.3	6
$\text{Fe}^{3+}/\text{TA}@\text{CF}$	1.30	77.2	7

PEHG	1.30	80.0	8
CNT modified filter paper	1.15	75.0	9
PDA/BNC aerogel	1.13	78.0	10
CNT@PAN	1.44	81.0	11
GO film	1.45	80.0	12
S-TiNO-800	1.49	89.1	13
Janus MXene- Based Aerogels	1.46	87.0	14
MXene-PVDF film	1.33	84.0	15
PVA-RGO gel	2.50	95.0	16
N-doped/ graphene/carbon hybrid aerogel	1.56	90.0	17
Au Nanoflowers- silica gel	1.36	85.0	18
Al NP-nanoporous membrane	~1	~58.0	19
PrGo	1.78	80.6	20
VA-GSM	1.62	86.5	21
d-Ti <sub>3</sub> C <sub>2</sub>	1.31	71.0	22
3D printing porous ceramic scaffold	1.53	84.2	23

---

MG@Silica/ceramic mesh	1.57	98	24
TiO <sub>2</sub> porous ceramics	2.05	/	25
Metal-ceramic carbide (ZrC)	1.43	98.2	26
TiN-Based Plasmonic Nanocomposites	1.76	99.1	27
CRHF/Au-NPs-10	1.22	84.0	28
TiN/FM	1.68	93.4	29
MoS <sub>2</sub> /PDMS	1.47	81.5	30
MnO <sub>2</sub> @PPy	1.69	88.1	31
CZTS NSAs	1.54	78.8	32
TiN-AAO	1.1	78.0	33
TiN/PVA/PVDF	1.0	66.7	34
<b>HPC@MPH</b>	<b>3.11</b>	<b>91.5</b>	<b>This work</b>

## References

- [1] K. Li, T. H. Chang, Z. Li, H. Yang, F. Fu, T. Li, J. S. Ho, P. Y. Chen, *Adv. Energy Mater.*, 2019, **9**, 1901687.
- [2] X. Ji, X. Fan, X. Liu, J. Gu, H. Lu, Z. Luan and J. Liang, *Nano Lett.*, 2024, **24**, 3498-3506.
- [3] M. Aizudin, M. K. Sudha, R. Goei, S. K. Lua, R. P. Pottammel, A. I. Y. Tok, E. H. Ang, *CHEM-EUR. J.*, 2023, **29**, e202203930.

- [4] H. Ren, M. Tang, B. Guan, K. Wang, J. Yang, F. Wang, M. Wang, J. Shan, Z. Chen, D. Wei, H. Peng, Z. Liu, *Adv. Mater.*, 2017, **29**, 1702590.
- [5] J. Hu, X. Yao, K. Han, Y. Ge, S. Xu, G. Bai, *Small*, 2024, **20**, 2405742.
- [6] W. Ruan, H. Zhang, J. Fu, Z. Li, J. Huang, Z. Liu, S. Zeng, Z. Chen, X. Li, Z. Yu, X. Liang, J. Ma, *Adv. Funct. Mater.*, 2024, **34**, 2312314.
- [7] Y. Zou, X. Wu, H. Li, L. Yang, C. Zhang, H. Wu, Y. Li, L. Xiao, *Carbohydr. Polym.*, 2021, **254**, 117404.
- [8] W. Zhao, H. Gong, Y. Song, B. Li, N. Xu, X. Min, G. Liu, B. Zhu, L. Zhou, X. X. Zhang, J. Zhu, *Adv. Funct. Mater.*, 2021, **31**, 2100025.
- [9] P. Yang, K. Liu, Q. Chen, J. Li, J. Duan, G. Xue, Z. Xu, W. Xie, J. Zhou, *Energ Environ. Sci.*, 2017, **10**, 1923.
- [10] Q. Jiang, H. Gholami Derami, D. Ghim, S. Cao, Y.-S. Jun, S. Singamaneni, *J Mater. Chem. A.*, 2017, **5**, 18397.
- [11] B. Zhu, H. Kou, Z. Liu, Z. Wang, D. K. Macharia, M. Zhu, B. Wu, X. Liu, Z. Chen, *ACS Appl. Mater. Inter.*, 2019, **11**, 35005.
- [12] X. Li, W. Xu, M. Tang, L. Zhou, B. Zhu, S. Zhu, J. Zhu, P. *Natl. Acad. Sci. USA.*, 2016, **113**, 13953.
- [13] X. Cheng, X. Bai, J. Yang, X. M. Zhu, J. Wang, *ACS Appl Mater. Inter.*, 2022, **14**, 28769–28780.

- [14] Q. Zhang, G. Yi, Z. Fu, H. Yu, S. Chen, X. Quan, *ACS Nano*, 2019, **13**, 13196.
- [15] R. Li, L. Zhang, L. Shi, P. Wang, *ACS Nano*, 2017, **11**, 3752.
- [16] X. Zhou, F. Zhao, Y. Guo, Y. Zhang, G. Yu, *Energy Environ. Sci.*, 2018, **11**, 1985.
- [17] B. Huo, D. Jiang, X. Cao, H. Liang, Z. Liu, C. Li, J. Liu, N-doped graphene /carbon hybrid aerogels for efficient solar steam generation. *Carbon*, 2019, **142**, 13-19.
- [18] M. Gao, C. K. Peh, H. T. Phan, L. Zhu, G. W. Ho, *Adv. Energy Mater.*, 2018, **8**, 1800711.
- [19] L. Zhou, Y. L. Tan, J. Wang, W. Xu, Y. Yuan, W. Cai, S. Zhu, J. Zhu, *Nat. Photon.*, 2016, **10**, 393.
- [20] Z. Wang, Q. Ye, X. Liang, J. Xu, C. Chang, C. Song, W. Shang, J. Wu, P. Tao, T. Deng, *J Mater. Chem. A.*, 2017, **5**, 16359.
- [21] P. Zhang, J. Li, L. Lv, Y. Zhao, L. Qu, *ACS Nano*, 2017, **11**, 5087.
- [22] J. Zhao, Y. Yang, C. Yang, Y. Tian, Y. Han, J. Liu, X. Yin, W. Que, *J Mater. Chem. A.*, 2018, **6**, 16196.
- [23] X. Zhou, M. Guo, M. Huang, Y. Xu, M. Liu, *Chem. Eng. J.*, 2024, **501**, 157659.

- [24] W. Jonhson, X. Xu, D. Zhang, W. Chua, Y. Tan, X. Liu, C. Guan, X. Tan, Y. Li, T. S. Heng, J. C. H. Goh, J. Wang, H. He, J. Ding, *ACS Appl. Mater. Interfaces* 2021, **13**, 23220–23229.
- [25] L. Chen, D. Yao, H. Liang, Y. Xia, Y. Zeng, *Energy Technol.*, 2023, **11**, 2300430.
- [26] S. Ai, M. Ma, Y. Chen, X. Gao, G. Liu, *Chem. Eng. J.*, 2022, **429**, 132014.
- [27] Y. Wang, X. Liu, Q. Zhang, C. Wang, S. Huang, Y. Liu, T. Yu, R. Yang, G. Z. Chen, M. Chaker, D. Ma, *Adv. Funct. Mater.*, 2023, **33**, 2212301.
- [28] W. Fang, H. Chen, X. He, W. Li, W. Zhang, Y. Shen, X. Chen, L. Zhao, *J. Porous Mater.*, 2021, **28**, 1655–1666.
- [29] Y. Gao, X. Zhou, N. Fu, S. Su, B. Ma, Q. Ruan, D. Wu, N. Zhang, Z. Deng, R. Jiang, *Chem. Eng. J.*, 2023, **475**, 146078.
- [30] J. Jiang, H. Jiang, Y. Xu, L. Ai, *Desalination*, 2022, **539**, 115943.
- [31] M. S. Irshad, X. Wang, N. Arshad, M. Q. Javed, T. Shamim, Z. Guo, H. Li, J. Wang, T. Mei. *Sci. Nano*, 2022, **9**, 1685-1698.
- [32] J. Zhang, Y. Yang, J. Zhao, Z. Daia, W. Liu, C. Chen, S. Gao, D.A. Golosov, S. M. Zavadski, S. N. Melnikov, *Mater. Res. Bull.*, 2019, **118** 110529.

[33] E. Traver, R. A. Karaballi, Y. E. Monfared, H. Daurie, G. A. Gagnon, M. Dasog , *ACS Appl. Nano Mater.*, 2020, **3**, 2787-2794.

[34] M. U. Farid, J. A. Kharraz, A. K. An, *ACS Appl. Mater. Interfaces.*, 2021, **13**, 3805-3815.